Biomedical Signal Processing and Control 62 (2020) 102099

Contents lists available at ScienceDirect

Biomedical Signal Processing and Control

journal homepage: www.elsevier.com/locate/bspc

Diagnostic prediction of autism spectrum disorder using complex network measures in a machine learning framework

N. Chaitra [a,b,*], P.A. Vijaya [a,b], Gopikrishna Deshpande [c,d,e,f,g,h,i,j]

[a] Department of Electronics and Communication Engineering, BNM Institute of Technology, Bangalore, India
[b] Visvesvaraya Technological University, Belagavi, Karnataka, India
[c] AU MRI Research Center, Department of Electrical and Computer Engineering, Auburn University, Auburn, AL, USA
[d] Department of Psychology, Auburn University, Auburn, AL, USA
[e] Alabama Advanced Imaging Consortium, Birmingham, AL, USA
[f] Center for Neuroscience, Auburn University, AL, USA
[g] Center for Health Ecology and Equity Research, Auburn University, Auburn, AL, USA
[h] School of Psychology, Capital Normal University, Beijing, China
[i] Key Laboratory for Learning and Cognition, Capital Normal University, Beijing, China
[j] Department of Psychiatry, National Institute of Mental Health and Neurosciences, Bengaluru, India

ARTICLE INFO

Keywords:
Autism spectrum disorder
Resting-state fMRI
Complex network measures
Machine learning
Support vector machine
Functional connectivity

ABSTRACT

Objective imaging-based biomarker discovery for psychiatric conditions is critical for accurate diagnosis and treatment. Using a machine learning framework, this work investigated the utility of brain's functional network topology (complex network features) extracted from functional magnetic resonance imaging (fMRI) functional connectivity (FC) as viable biomarker of autism spectrum disorder (ASD). To this end, we utilized resting-state fMRI data from the publicly available ABIDE dataset consisting of 432 ASD patients and 556 matched healthy controls. Upon standard pre-processing, 3D + time fMRI data were parcellated into 200 functionally homogenous regions, and whole-brain FC network using Pearson's correlation was obtained from corresponding regional mean time series. A battery of complex network features were computed from the FC network using graph theoretic techniques. Recursive-Cluster-Elimination Support Vector Machine algorithm was employed to compare the predictive performance of three independent feature sets, (i) FC, (ii) complex network measures, and (iii) both combined. The study found that FC could diagnose ASD with 67.3 % accuracy and graph measures with 64.5 % accuracy, while the combined feature set could diagnose with 70.1 % accuracy (all accuracies were significantly different, $p < 10^{-30}$). The most discriminative imaging features were mainly from lateral temporal, occipital, precuneus (all reduced in ASD) and orbito-frontal (elevated in ASD) regions. We concluded that network topology (graph measures) carried some unique information about ASD pathology not available in bivariate connectivity (FC), and that using both together provided better prediction than using individual measures. Future prediction studies could incorporate multiple fMRI analysis strategies within their framework to achieve superior prediction performances.

1. Introduction

Autism spectrum disorder (ASD) is a neurodevelopmental disorder which affects an estimated 24.8 million people worldwide [1]. It is characterized by difficulty in communication and deficits in social interaction, coupled with highly repetitive patterns of interests and behavior. Symptoms of ASD manifest early in childhood and can lead to significant functional impairment. Therefore, early and accurate diagnosis is especially important towards improving quality of life, decrease symptom severity and maladaptive behaviors.

Despite intense research, the neural mechanisms of ASD are not clearly understood. Consequently, diagnosis of ASD is based on behavior, and not the cause or mechanism [2]. Genetic tests are widely used to identify specific genetic causes once ASD is diagnosed, but genetic tests are only an indicator of potential risk and not diagnosis. On the other hand, substantial research progress has been made in the past

* Corresponding author at: Department of Electronics and Communication Engineering, BNM Institute of Technology, 12th Main, 27th Cross, Banashankari 2nd Stage, Bangalore 560070, Karnataka, India.
E-mail address: chaitranagraj@gmail.com (N. Chaitra).

https://doi.org/10.1016/j.bspc.2020.102099
Received 11 December 2019; Received in revised form 9 July 2020; Accepted 21 July 2020
Available online 18 August 2020

two decades characterizing ASD at the systems-level using brain imaging techniques. Yet, it has not been used as a standard tool in the diagnosis of ASD.

1.1. Functional MRI and autism spectrum disorder

Functional magnetic resonance imaging (fMRI) has emerged as a powerful tool for characterizing brain function in health and disease. Despite the wealth of fMRI data from individuals with ASD, our understanding of how ASD manifests functionally is nascent. Identifying sensitive and specific biomarkers for ASD from fMRI data could not only be helpful in diagnosis, but also be useful in prognosis and treatment. Furthermore, if the biomarkers are quantitative, then one can also use them as metrics for efficacy of behavioral or pharmacologic interventions. In this light, there has been a significant body of literature on understanding specific biomarkers for ASD using fMRI data. We will briefly survey a few here.

Although there are known local functional or structural brain abnormalities in ASD, studies suggest that these alone do not capture all the relevant dimensions of ASD. Specifically, research suggests that there are relevant markers for ASD embedded in atypical connectivity among regions of the brain, in addition to structural or anatomical irregularities [3–5]. This poses a significant challenge to identifying specific markers for ASD and understanding the mechanism given that brain connectivity is expansive and multidimensional in nature.

1.2. FMRI connectivity in autism spectrum disorder

Decreased functional connectivity (FC) in ASD was first reported by three independent groups [6–8], and has since been confirmed by more than 50 primary reports obtained from fMRI data of resting state and while performing cognitive tasks [9]. Most of the studies show decrease in brain connectivity, including brain's default mode network's nodes [10–12], social brain regions [13,14], attentional regions [15], language regions [16], inter-hemispheric homologues [17], and elsewhere in the brain [18]. However, there are also reports that show abnormal increases in FC [19] or unchanged connectivity [20]. Specifically, negative connections [18], corticostriatal connections [21], visual search regions [22], and brain network-level metrics [23,24] have shown higher absolute connectivity value in ASD. Taken together, there appears to be a dichotomy in connectivity patterns with some networks exhibiting elevated connectivity and some others exhibiting otherwise, although not all studies clearly agree with each other. In summary, some useful biomarkers for ASD lay in the complex connectivity relationships between various parts of the brain. Further, it is difficult to summarize the abnormalities as decreased or increased connectivity between specific, but limited number of areas, but seem to involve a complicated pattern of changes that span large parts of the brain.

1.3. Complex network analysis using fMRI connectivity

Although such observations have been made on bivariate relationships between brain regions (i.e. pairwise FC), another school of thought has emerged in recent years wherein ensemble of connections are studied by quantifying their network structure instead. This approach, called complex network modeling [25], studies the brain from a different perspective and is considered to quantify some unique characteristics about brain networks not available through conventional connectivity. It can inform us about patterns within the connectivity network, and this has been shown to be sensitive to disease pathology in several disorders [26,27]. It also provides novel mechanistic information not available through just FC [28].

Complex network analysis relies on characterizing brain networks in terms of graph theory. A graph consists of a set of nodes and links connecting the nodes, possibly with weights associated with the links; in our context, brain regions are the nodes and connectivity weights are the links. Graph theory is a vast discipline with a plethora of applications to numerous fields of science [29,30]. Graph theoretic techniques such as spectral clustering have been long used for parcellation to create brain atlases [31]. However, more recently, Rubinov and Sporns [25] introduced use and analysis of complex-network measures in brain imaging. Graph theoretic notions have since been used to study mental illnesses [26,27]. Specifically with respect to ASD, many studies [32–34] have examined the potential of complex network features using imaging datasets obtained from those with ASD. However, there hasn't been a comprehensive analysis of the relative importance of all the different complex network measures as well as traditional FC using a large dataset in autism. In this study, we used an analysis framework consisting of a combination of traditional connectivity modeling and complex network modeling.

1.4. Motivation for using machine learning to identify ASD biomarkers

As mentioned earlier, identifying objective imaging-based biomarkers is the central aim of this study, and to this end we sought to identify connectivity and complex network biomarkers of ASD. In this study, we assessed the relative ability of traditional connectivity and complex network measures in diagnosing ASD at the individual subject level. Additionally, since complex network measures quantify some unique information about brain function not available through traditional connectivity [35], a framework comprising of both connectivity and complex network measures might be able to diagnose ASD better than each of them individually; hence, we assessed the combined feature set in a similar manner. In all these assessments, our goal was to diagnose ASD at the individual subject level, which is not achievable through population-level statistical analyses. Hence, as in previous studies [36,37], we used a machine learning framework in this study. Specifically, classification accuracy obtained through machine learning classification was used as the yardstick to compare the relative diagnostic efficacy of traditional connectivity and complex network features.

1.5. Literature review of machine learning applied to fMRI data to study ASD

So far, we described the motivation for studying autism using fMRI (specifically connectivity), and how complex network measures derived from FC could provide additional insights. We then described the motivation for using machine learning as a framework to assess FC and complex network measures as predictors of ASD. Next, we will briefly describe prior literature on machine learning applied to fMRI data in general and then ASD in particular. Machine learning methods have been applied on brain imaging datasets for a wide variety of applications. For example, they have been used to classify mental states related to representation of semantic groups [38,39], of the meanings of nouns [40–42], of emotions [43], for predicting purchase decisions [44], inter-personal trust [45], and of learning [46]. Similarly, machine learning techniques have been used to identify brain activations associated with schizophrenia [47], depression [48], ADHD and PTSD [49–51].

There have been several works that have applied machine learning techniques towards diagnosing ASD [52]. Nielsen et al. [53] obtained 60 % accuracy for classifying ASD from controls using publicly available Autism Brain Imaging Data Exchange (ABIDE) dataset. More recently, Abraham et al. [54] built on participant-specific FC matrices and they attained 67 % classification accuracy for complete ABIDE dataset. Gori et al. [55] extracted features from subregions of the gray matter, and used those to identify ASD from controls. Using a multi-kernel support vector machine (SVM) classification method, Jin et al. [56] obtained a classification accuracy of 76 %. On smaller datasets Chen et al. [57] and Odriozola et al. [58] obtained classification accuracies of 79.17 % and 85 % respectively. Using the method of support vector machine and recursive feature elimination on data under social stimuli (not

resting-state fMRI), Chanel et al. [59] have pushed the accuracy all the way up to 92.3 %. Finally, by utilizing deep neural networks towards the classification task [60], a 70 % accuracy on the same dataset was achieved. Perhaps, the work closest to ours is that of [32] who introduced a technique called random SVM cluster, and used it in conjunction with a limited graph-theoretic feature set, to achieve an accuracy of over 90 %. Libero et al. used multimodal data to perform ASD classification [61]. However, overfitting can be a huge confound in studies employing small datasets since it leads to inflated estimates of accuracy [62,63].

1.6. Machine learning technique employed and how it was used to achieve our aims

With this background, we next describe the specific technique employed by us. Our study utilized a recursive cluster elimination (RCE) based support vector machine (SVM) technique to perform machine learning classification to evaluate the predictive ability of traditional connectivity and complex network measures obtained from the ABIDE dataset. SVMs are a class of classifiers that not only have a sound theoretical underpinning but are also applied in a wide variety of application areas. RCE is a simple and effective iterative procedure to select relevant features from a large feature set. RCE in conjunction with SVMs have been used successfully in earlier works [36].

After appropriate preprocessing, a network of FC was constructed for each individual, and a variety of graph-theoretic features were extracted for use in the machine learning framework to classify ASD from controls. We performed classification separately with three distinct feature sets: with *(i) connectivity features alone, (ii) complex network (graph) measures alone, and (iii) a feature set comprising of both connectivity and graph measures*. We compared results from the three feature sets, and as mentioned previously our yardstick for the diagnosing ability of the features was the classification accuracy. Given that graph measures and conventional connectivity measures contain some proportion of mutually unique information [25], *we hypothesized that we would obtain the best classification with the combined feature set*. Qualitatively, classification performance is directly proportional to the amount of information we have about the class distinctions, hence our hypothesis banks on the idea that graph measures and connectivity will have an additive effect on the classification performance. Finally, the RCE-SVM subroutine was used to *identify a subset of input features that had the highest ability in diagnosing ASD*, based on the classification performance.

1.7. Importance of our study

This is one of the first studies that tries to assess complex network features in the RCE-SVM framework as diagnostic markers of ASD, as well as to compare traditional connectivity and complex network measures in ASD within the same model. Although there have been studies that have applied machine learning techniques towards classifying ASD from controls, the usefulness of complex network measures as in a combined feature set has not been investigated before.

Our study contributes further to the body of literature on using brain imaging data for the diagnosis of ASD using machine learning. With the ABIDE data set itself, earlier studies have applied various machine learning techniques ranging from SVMs to neural networks [60], and have reported classification accuracies ranging from 65 % to 70 %. Although our best accuracy might be lower than some reported in previous studies, it is possibly due to the fact that some studies only used a smaller dataset or used a subset of ABIDE data (as mentioned before, smaller data sets overfit the data leading to inflated performance measures [62,63]). In our study, comparing different machine learning techniques for classification was not the aim, nor was our aim to obtain the best accuracy across all previously published studies. Rather our goal was to assess different feature sets, particularly a combined feature set of connectivity and graph measures, and we used RCE-SVM outcome merely as a yardstick for that comparison. Very few studies have given attention to the comparison of different feature sets, while larger interest has previously been on the machine learning techniques instead.

1.8. Organization of the paper

The following sections describe the process we followed to carry out our research in detail. Information about the dataset, and preprocessing procedure employed are described in the methods section, which is followed by details about FC and complex network analysis along with RCE-SVM method for machine learning classification analysis to assess the classification performance of the three different feature sets. Methods section is followed by results, discussion and conclusion.

2. Methods

2.1. Participants

We used the publicly available ABIDE preprocessed dataset for our study [64]. The ABIDE dataset is a collection of brain imaging data of 1112 individuals of which 539 are individuals with ASD (includes autism and Asperger's syndrome), and 573 are age-matched typical controls. This dataset is an aggregation of 20 previously collected datasets from seventeen sites. For each individual, the dataset contains fMRI acquisitions along with structural MRI and phenotypic information. In accordance with HIPAA guidelines, data is completely anonymized. Information regarding acquisition, protocols and informed consent are described in Ref. [65]. Information about phenotypic information (age, sex, handedness, IQ and diagnostic details) is also available there.

The samples have a huge majority of males, with 25 % of seventeen contributing sites excluding females, owing to higher male predominance of ASD. Complete and verbal IQ were considerably higher for typical controls than Autistic individuals ($p < 0.0001$) and also performance IQ was higher, although it varied marginally ($p = 0.067$). We refer the reader to Ref. [65] for detailed information about the methods used by the sites to reach ASD diagnosis, their reliability, and other information about the dataset.

2.2. FMRI data pre-processing

The preprocessing procedure used in the ABIDE preprocessed dataset is described in detail in Ref. [65]. Here we briefly describe some of the key highlights. Data Processing Assistant for Resting-State MRI (DPARSF) software was used for preprocessing of resting-state fMRI. The preprocessing steps began with slicing time correction, realignment and co-registration to standard MNI space. This was followed by nuisance signal regression to minimize variation because of physiological processes such as respiration, heartbeat, head motion, along with low frequency scanner drifts in the fMRI signal.

Blind deconvolution was carried out to reduce non-neural variability because of hemodynamic response function (HRF) [66]. Recent research shows that HRF variability confounds fMRI connectivity estimates by as much as 15 % [67,68]; these authors recommend deconvolution to mitigate the issue. This is also true in specific mental health disorders [69,70], including ASD [71,72]. Deconvolution was performed with the method suggested by Wu et al. [73] using Matlab scripts by Wu et al., which provided us latent neuronal time series. Hemodynamic response function and latent neural time series are not measured, but are estimated from the data, which necessitates blind deconvolution. This deconvolved data was used in further analysis. Craddock et al. 200-region brain parcellation (popularly called the CC200 atlas) [31] was used towards specifying regions of interest (ROI) in the fMRI data. The CC200 atlas consists of 200 functionally homogenous brain regions obtained using spectral clustering. Each of these 200 ROIs consisted of about 1000 voxels that had homogenous connectivity properties in resting-state, and together these 200 ROIs encompassed all voxels in the

brain's gray matter including cerebral cortex, sub cortex, midbrain and cerebellum. A mean time series was obtained for each of these 200 ROIs for each subject, which was the starting point for our FC analysis.

2.3. Functional connectivity analysis

The time series associated with every ROI was normalized to make it mean zero and unit variance. FC was calculated between every pair of ROIs with Pearson's correlation coefficient (PCC), providing us a 200×200 connectivity matrix for each participant. This was used to construct a graph for each subject, with the absolute connectivity weights being the edges of the graph, and the 200 ROIs being the nodes. We used weighted connectivity matrices for deriving complex network measures due to issues arising from binarizing the matrices [25].

2.4. Complex-network analysis

Starting with the graphs extracted from FC, a variety of graph-theoretic features were computed for each individual. In the context of brain imaging, the relevant graph-theoretic measures can be used to quantify various aspects of brain function such as functional integration, functional segregation, resilience and importance of individual nodes. The list of graph-theoretic measures used in this study is provided in Table 1.

We refer the reader to Ref. [25] for a formal description of the measures obtained from complex network (or graph-theoretic) analysis. Here we will briefly describe the complex network measures used in this study as features for machine learning classification.

Node or vertex degree of a node is the number edges connected to that node which is nothing but the total number of neighbors of the node. Node strength is the total of all the weights of edges connected to the node under consideration.

2.4.1. Measures of centrality

Measures node and edge centrality evaluate the significance of individual nodes and edges in the given network. The simplest measure for node centrality is the degree of the node, which gives the number of connections the node has with other nodes. Nodes having high degree interact with several other nodes, and are therefore considered to be important for the functioning of the network.

A more sophisticated measure of centrality is node and edge betweenness centrality. Node betweenness centrality characterizes the number of the shortest paths of the network that run through the given vertex or the node. Edge betweenness centrality is defined as the number of all the shortest paths that comprise of a given edge. Edges having higher values of betweenness centrality contribute to a greater number of shortest paths.

In networks where the nodes are further divided into modules, within and between-module connectivity degree-based measures are considered [74]. The within-module degree z-score is a localized form of degree centrality. The variety of intermodular interconnections of individual nodes are assessed by complementary participation coefficient. Those having high within-module degree and low participation coefficient, also called as provincial hubs, are considered to play a critical role in the facilitation of modular segregation. Connector hubs which are nodes having high participation coefficient enable global inter-modular integration. Next, we describe the complex network measures that characterize segregation and integration.

Table 1
List of complex network measures used as features in this study.

Network measure	Dimensions	Parameters and comments
Node degrees	200×1	
Node strengths	200×1	
Node betweenness centrality	200×1	
Edge betweenness centrality	200 x 200,	Betweenness for each edge of the network
Clustering coefficient	200×1	
Transitivity	1×1	
Modularity	200×1	Resolution parameter default = 1
Degree z-score	200×1	Degree centrality within the partition computed above
Participation coefficient	200×1	Participation coefficients for the participation computed above
Louvain modularity partition	200×1	
Consensus	200×1	Threshold = 0.1 Number of reclusterings — 9
Characteristic path length	1×1	
Global Efficiency	1×1	
Assortativity	1×1	
Rich Club Coefficient	200×1	Max level unspecified, equal to max degree = 200
Eccentricity	200×1	
Radius	1×1	
Diameter	1×1	

2.4.2. Measures of functional segregation and integration

Grouping of brain regions into densely connected clusters can be referred to as functional segregation. Each of the cluster could specialize in one or more brain functions. Measures for segregation mainly quantifies the occurrence of groups, also called as modules or clusters, inside the given network.

Clustering coefficient refers to the proportion of triangles around an individual node. It also refers to the section of neighbors of a node which are neighbors to each other [75]. The average clustering coefficient of the nodes of the network is given by the mean clustering coefficient. A modified version of the clustering coefficient called as transitivity normalizes the number of triangles over the entire graph, and hence it is not disproportionately affected by low-degree vertices.

Community structure of a network comprises of partitioning of the network into groups of nodes to maximize the intra-community links and minimize the links between communities. Community structure is not individually determined or easily computable. Therefore, community structure is often computed with an optimization procedure. Modularity is used to measure how amenable the network is to the partition into communities. Louvain modularity partition is calculated using Louvain method of detecting communities in networks which aids in maximizing the modularity. Consensus partitioning provides one consensus partition of degenerate partitions.

Complementary to segregation, combining specialized information from several regions of the brain is called functional integration. Measures of integration depict the same by assessing the ease with which regions of the brain communicate with each other. Characteristic path length gives the average of all the shortest path lengths between all the pair of nodes in a given network. It is calculated by taking the average distance from a certain vertex to every other vertex. That is:

$$d_v = \frac{1}{|V(G)| - 1} \cdot \sum_{v \neq w} d(v, w) \tag{1}$$

After doing it for every vertex $v \in V(G)$, median is calculated for all previously calculated d_v. Global efficiency is the average inverse shortest path length [76]. Roughly speaking, the characteristic path length is mainly influenced by long paths and global efficiency by short paths. The node eccentricity gives the largest shortest path length between two given nodes. Radius and diameter give minimum and maximum eccentricity respectively.

2.4.3. Measures of network resilience

The assortativity coefficient is a measure of resilience given by the correlation coefficient between the nodes at two opposite ends of a connection. Positive assortativity coefficient for a network demonstrates

resilient core of mutually connected high-degree hubs. Negative assortativity coefficient for a network indicates widely distributed and weak high-degree hubs. Rich club coefficient at level D gives the fraction of edges that connect nodes of degree D or higher than that of maximum number of edges that such nodes are allowed to share.

In summary, we used a combined set of the following graph measures for classification analysis: Node degrees, strengths, node betweenness centrality, edge betweenness centrality, clustering coefficient, transitivity, modularity, degree z-score, participation coefficient, Louvain modularity partition, consensus, characteristic path length, global efficiency, assortativity, rich club coefficient, eccentricity, radius and diameter.

2.5. Machine learning classification analysis

The large graph-theoretic feature set listed in Table 1 as well as the traditional FC data were used as features in the RCE-SVM framework. First, a two-sample *t*-test was performed between ASD and controls ($p < 0.05$, uncorrected) for FC data as well as for each graph measure. This was performed only in the training data to reduce the number of input features to choose the most relevant features for classification, which has been shown to improve classification performance [48] by assuring that non-discriminatory features would not be used in the classifier. As noted earlier, classification was performed separately and compared using three distinct feature sets, wherein the features were obtained in the fashion mentioned above. (i) Feature set-1: FC features, (ii) feature set-2: all complex network features obtained using the approach mentioned above and then concatenated together to form one set, and (iii) feature set-3: a concatenation of feature sets 1 and 2. These features were then used as inputs to the classification. We briefly review the RCE-SVM technique below.

2.5.1. RCE-SVM method

The RCE-SVM method was introduced by Yousef et al. [77]. The central algorithm of RCE SVM mainly consists of three steps: the Cluster step to cluster the features, the SVM scoring step to compute the importance of every cluster of features towards classification and the RCE step for removing clusters having lower score, which is carried out as explained below:

Consider a dataset N where each data point has F features. The dataset is divided into two parts, training (90 % of the data) and testing (10 % of the data) datasets. Let $N1$ denote training dataset and F denote features. For any subset of features A, i.e., $A \subseteq F$, let us define a score as their ability to distinguish the two classes with SVM. To compute the score, the training set is randomly partitioned. That is samples $N1$ is divided into k subsets, which are non-overlapping and are of equal sizes. SVM is trained using $k-1$ subsets. The one that remains is used to evaluate the performance. This process is iterated r number of times by partitioning randomly each time. $Score(N1(A),\ k,\ r)$ is the average accuracy of the SVM over the given dataset $N1$ which is denoted by its F features calculated over k-folds and with cross validation which is done r times. Let us make k to be equal to 6 and r to 100 as base values. If features F is grouped into sub-clusters $F_1, F_2, \ldots, F_n$ then the $Score(N1(F_i),\ k,\ r)$ is defined for every sub-cluster, where $N1(F_i)$ is nothing but the data $N1$ denoted by its features F_i. 20 % of the clusters with the lowest scores are removed and remaining features are merged into single pool. If the value of n, which denotes the number of sub-clusters of F, becomes less than or equal to 1, then the process is stopped otherwise it is continued till the termination criteria is reached. At each feature reduction step, the performance of the model for the test data is calculated and reported. This provides an estimate of how the test accuracy is changing across the feature reduction steps. The maximum test accuracy over all feature reduction steps is reported as the best model accuracy obtained.

Algorithm of RCE-SVM:

Input data: N1 = the training dataset

F = top features obtained from *t*-test (feature list)

n = number of clusters

d = 20 % (reduction parameter)

While ($n \leq 2$) repeat step 1–4.

1. Cluster step: Cluster the features F into n clusters $F_1,\ F_2, \ldots,\ F_n$ by K-means algorithm.
2. SVM scoring step: For every cluster $i\ =\ 1..n$, $Score(N1(F_i),\ k,\ r)$ is calculated.
3. RCE step: 20 % clusters with lowest score are removed
4. Combine remaining features into single pool.

Upon performing classification using the three feature sets separately, the best classification accuracies were compared across the feature sets to test our hypothesis. The top predictive features were assessed and interpreted within the framework of previously known neurobiological impairments in ASD (Fig. 1).

3. Results

Graph measures of functional segregation and integration were computed using connectivity networks, and traditional FC as well as graph measures were used in the RCE-SVM framework to assess these feature sets as capable biomarkers, assessed using classification accuracy. Classification accuracies obtained using connectivity features, using graph measures, as well as using a combined feature set comprising of both connectivity and graph measures were compared. It was found that connectivity alone resulted in 67.31 % accuracy in diagnosing ASD vs. controls, while graph measures resulted in 64.47 % accuracy. However, the combined feature set of connectivity + graph measures resulted in an accuracy of 70.01 %. Graph measures performed poorer than connectivity by about 3% ($p = 3.3 \times 10^{-62}$). The combined feature set performed better than traditional FC measures by about 3% ($p = 4.5 \times 10^{-61}$).

With FC, this best accuracy was obtained with 147 FC features (top predictors); while with graph measures 115 features were identified. In the case of combined features, 347 features (320 FC and 27 graph measures) were found. Although these large bunch of features resulted in the best classification performance, we narrowed our interpretation to

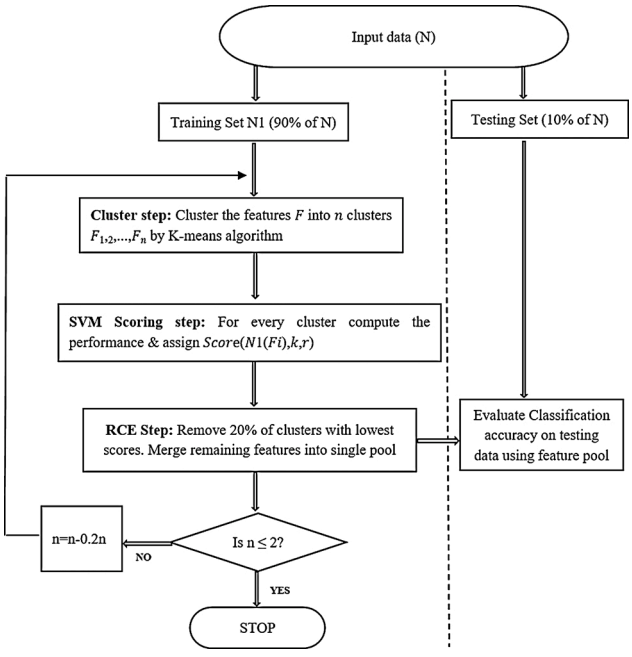

Fig. 1. Flow chart of the Recursive Cluster Elimination based Support Vector Machine (RCE-SVM) classification procedure.

a subset of those features that not only resulted in the best classification performance (predictive ability) but also had high statistical significance (ASD vs. controls, $p < 0.05$, corrected for multiple comparisons using the false discovery rate method). Such features having both statistical significance and predictive capability assume higher importance, we interpret our findings in light of these observations.

Table 2 lists the top predictive features using FC, while Table 3 lists them for graph measures. Table 4 lists the top predictive features for classification using the combined feature set.

In order to aid neuroscientific interpretation, Fig. 2 plots the features listed in Tables 2–4 on the brain using BrainNet Viewer [78]. Fig. 3 provides classification accuracies across RCE iterations for the three separate cases of feature sets. The figure also shows the highest accuracy obtained with each feature set. Table 5 summarizes the comparison of accuracies across the feature sets.

4. Discussion

This study investigated the efficacy of FC and complex network measures in diagnosing ASD vs. matched controls in a machine learning framework. We hypothesized that a feature set comprising of both connectivity and graph measures would diagnose ASD with better accuracy than with the individual feature sets alone, given that connectivity and graph measures are partially unique. To the best of our knowledge, this is among the first studies to assess such a combined feature set as a potential imaging tool for diagnosing ASD. We found evidence for our hypothesis as the combined feature set provided statistically significant higher accuracy than with either of the individual feature sets.

The study also established that complex network measures on their own do not yield better classification accuracy than traditional FC, at least in ASD with the ABIDE data set. This is also one of the first studies to assess complex network features in the RCE-SVM framework as diagnostic markers of ASD, as well as to compare connectivity and complex network measures in ASD. While there have been some studies applying machine learning techniques towards classifying ASD from controls, the utility of complex network measures in this context of a combined feature set has not been investigated. For example, there have been studies using complex network measures in ASD in the recent years [32–34], but they do not provide a comparative evaluation of complex network measures and traditional FC for classifying ASD.

Table 2
Top discriminative features identified by the RCE-SVM algorithm when functional connectivity alone was used as the feature set.

Sl. no.	Functional connectivity	MNI centroids of the two regions		p-Value	T-value[a]
1	Precuneus_R ↔ Frontal_Med_Orb_L	[13.3, −64.4, 24.0]	[1.4, 55.9, −7.2]	1.9×10^{-10}	6.44
2	Precuneus_R ↔ Frontal_Med_Orb_L	[13.3, −64.4, 24.0]	[−0.1, 38.9, −12.2]	5.4×10^{-7}	5.04
3	Precuneus_R ↔ Temporal_Mid_R	[13.3, −64.4, 24.0]	[55.1, −3.6, −25.4]	9.2×10^{-11}	6.55
4	Precuneus_R ↔ Temporal_Mid_R	[10.3, −63.5, 56.2]	[55.1, −3.6, −25.4]	0.0064	2.73
5	Frontal_Mid_Orb_L ↔ Temporal_Mid_L	[−28.3, 50.7, −11.6]	[−56.8, −48.2, 9.0]	0.0055	2.78
6	Frontal_Sup_R ↔ Temporal_Mid_L	[27.7, 58.2, −1.6]	[−56.4, −15.1, −15.3]	0.0051	2.81
7	Calcarine_L ↔ Temporal_Mid_R	[−9.9, −67.4, 22.4]	[55.1, −3.6, −25.4]	1.9×10^{-12}	7.13
8	Calcarine_L ↔ Temporal_Mid_R	[−9.9, −67.4, 22.4]	[61.9, −21.1, −15.6]	2.4×10^{-6}	4.74
9	Cuneus_R ↔ Temporal_Pole_L	[13.5, −77.4, 38.9]	[−40.6, 12.9, −28.2]	0.0329	2.14
10	Cuneus_R ↔ Temporal_Inf_L	[13.5, −77.4, 38.9]	[−51.0, −3.6, −28.8]	0.0049	2.82
11	Cuneus_R ↔ Cingulum_Mid_R	[13.5, −77.4, 38.9]	[9.1, −35.9, 47.1]	0.0048	−2.83
12	Cuneus_R ↔ Fusiform_R	[13.5, −77.4, 38.9]	[34.0, −31.4, −16.4]	0.0084	2.64
13	Fusiform_L ↔ Frontal_Inf_Orb_R	[−30.5, −5.1, −32.6]	[44.6, 29.2, −9.5]	0.0387	2.07

[a] Controls > ASD: positive T-value; ASD > Controls: negative T-value.

Table 3
Top discriminative features identified by the RCE-SVM algorithm when complex network measures alone were used as the feature set.

Sl. no.	Graph measure	Region name	MNI centroid of region	p-Value	T-value[a]
1	Modularity consensus partition score	Temporal_Pole_R	[43.5, 9.9, −36.2]	4.5×10^{-6}	−4.61
2	Modularity consensus partition score	Temporal_Inf_L	[−51.0, −3.6, −28.8]	4.2×10^{-4}	−3.54
3	Modularity consensus partition score	Temporal_Mid_L	[−56.4, −15.1, −15.3]	3.6×10^{-4}	−3.58
4	Modularity consensus partition score	Temporal_Inf_L	[−38.9, 5.7, −39.4]	2.1×10^{-5}	−4.28
5	Modularity consensus partition score	Occipital_Inf_L	[−35.8, −78.1, −14.9]	0.0018	−3.14
6	Within-Module Degree Z-score	Precuneus_L	[−3.9, −53.1, 57.4]	7×10^{-7}	−4.99
7	Within-Module Degree Z-score	Precuneus_L	[−7.6, −74.8, 41.1]	0.0037	−2.91
8	Within-Module Degree Z-score	Precuneus_R	[10.3, −63.5, 56.2]	1.4×10^{-6}	−4.87

[a] Controls > ASD: positive T-value; ASD > Controls: negative T-value.

4.1. Importance of higher classification accuracy with combined feature set

The improvement in classification accuracy reported using the combined feature set is certainly significant and impactful, in our opinion. Specifically, for every 100 automated diagnoses of ASD using fMRI and machine learning, our study shows that the combined feature set can correctly diagnose about 3 people more as compared to a diagnosis using conventional FC feature sets. We believe that it is such advancements, piled over time, that ultimately help in translating research-domain results into clinical care. In fact, the National Institutes of Health (NIH) of the United States of America has endorsed such a view through the promotion and advocacy of the Research Domain Criteria (RDoC, http://www.nimh.nih.gov/research-priorities/rdoc/nimh-research-domaincriteria-rdoc.shtml), which involves objective diagnosis of mental disorders using brain imaging data and network modeling using “circuits” as a “unit of analysis”, as well as computational approaches such as machine learning. Not only does the study establish the importance of using complex network features as part of the feature set, it also identifies the most relevant features using the RCE-SVM framework.

Table 4
Top discriminative features among both functional connectivity and complex network measures when both are used as features in the RCE-SVM algorithm.

Sl. no.	Measure	Connections (regions)	MNI centroids		p-Value	T-value[a]
1	Functional Connectivity	Frontal_Med_Orb_L ↔ Frontal_Inf_Orb_L	[−0.1, 38.9, −12.2]	[−44.0, 33.0, −8.1]	0.0002	−3.65
2	Functional Connectivity	Frontal_Mid_R ↔ Cingulum_Ant_L	[31.7, 54.8, 14.9]	[−6.8, 45.7, 7.8]	0.0031	−2.97
3	Functional Connectivity	Caudate_L ↔ Temporal_Pole_L	[−13.8, 12.6, −2.9]	[−40.6, 12.9, −28.2]	5.4×10^{-7}	5.04
4	Functional Connectivity	Caudate_R ↔ Frontal_Inf_Tri_R	[13.5, 12.3, −7.0]	[52.1, 28.0, 4.9]	0.0002	−3.68
5	Functional Connectivity	Caudate_R ↔ Frontal_Inf_Orb_R	[13.5, 12.3, −7.0]	[44.6, 29.2, −9.5]	0.0003	−3.61
6	Functional Connectivity	Fusiform_L ↔ Frontal_Inf_Orb_R	[−30.5, −5.1, −32.6]	[44.6, 29.2, −9.5]	0.0387	2.07
7	Functional Connectivity	Precuneus_R ↔ Frontal_Med_Orb_L	[13.3, −64.4, 24.0]	[−0.1, 38.9, −12.2]	1.9×10^{-12}	7.13
8	Functional Connectivity	Precuneus_R ↔ Frontal_Med_Orb_L	[13.3, −64.4, 24.0]	[1.4, 55.9, −7.2]	0.0488	1.97
9	Functional Connectivity	Precuneus_R ↔ Temporal_Mid_R	[13.3, −64.4, 24.0]	[55.1, −3.6, −25.4]	1.8×10^{-10}	6.44
10	Functional Connectivity	Calcarine_L ↔ Temporal_Mid_R	[−9.9, −67.4, 22.4]	[61.9, −21.1, −15.6]	4×10^{-5}	−4.13
11	Functional Connectivity	Calcarine_L ↔ Temporal_Mid_R	[−9.9, −67.4, 22.4]	[55.1, −3.6, −25.4]	0.0084	2.64
12	Functional Connectivity	Calcarine_R ↔ Cuneus_R	[13.5, −94.4, 2.2]	[13.5, −77.4, 38.9]	0.0003	−3.61
13	Functional Connectivity	Calcarine_L ↔ Frontal_Mid_R	[−9.9, −67.4, 22.4]	[28.6, 34.6, 42.0]	0.0397	2.06
14	Functional Connectivity	Fusiform_R ↔ Cuneus_R	[34.0, −31.4, −16.4]	[13.5, −77.4, 38.9]	2.4×10^{-6}	4.74
15	Functional Connectivity	Calcarine_L ↔ ParaHippocampal_L	[−9.9, −67.4, 22.4]	[−15.0, −30.8, −18.3]	9.2×10^{-11}	6.55
16	Within-Module Degree Z-score	Precuneus_L	[−3.9, −53.1, 57.4]		7×10^{-7}	−4.99

[a] Controls > ASD: positive T-value; ASD > Controls: negative T-value.

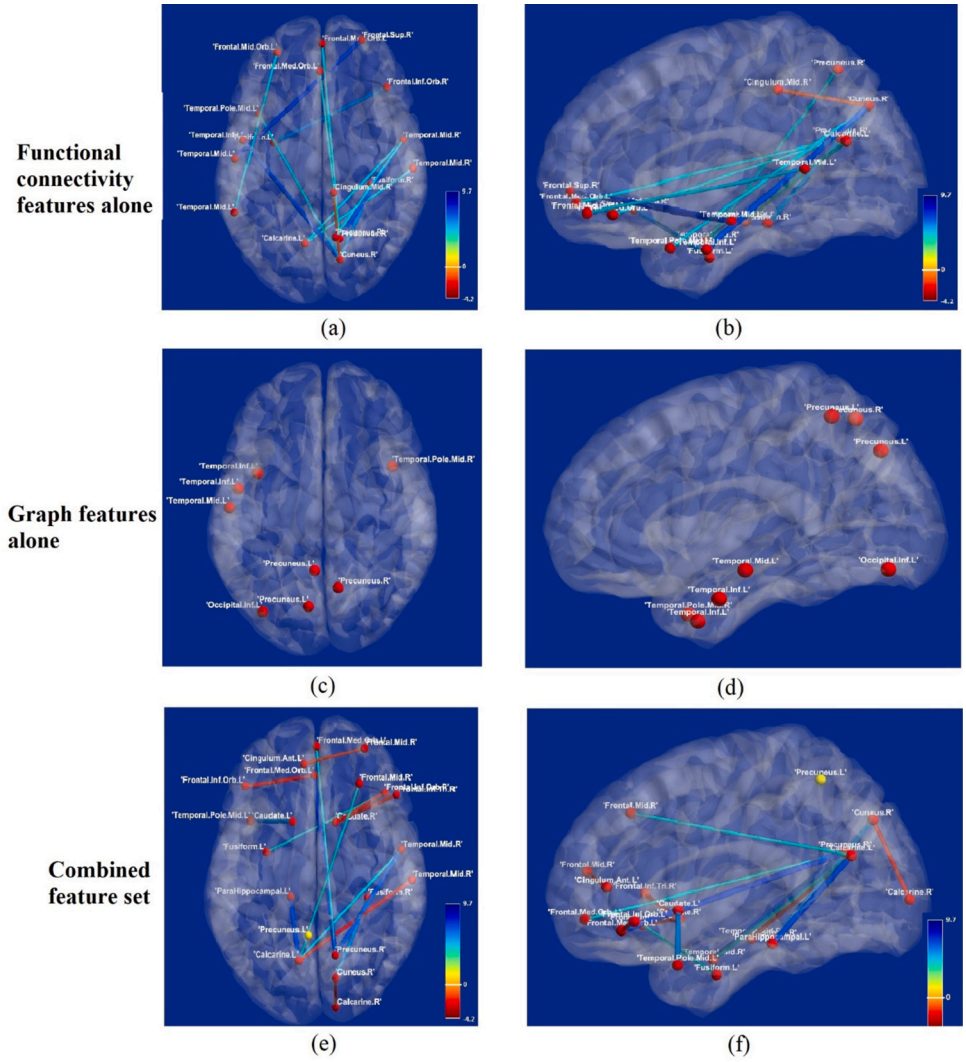

Fig. 2. Brain connectivity map of top-predictive features obtained through RCE-SVM classification (that were also statistically significant between groups, $p < 0.05$, FDR corrected) with (i) top row: functional connectivity features alone (a. axial view b. sagittal view), (ii) middle row: complex network features alone (c. axial view d. sagittal view) and (iii) bottom row: combined feature set (e. axial view f. sagittal view). Red connections were higher in ASD vs. controls and blue ones higher in controls vs. ASD. In the combined feature set image (e and f), red regions/nodes were associated with functional connectivity while the sole yellow region of left precuneus was a nodal complex network measure (specifically, Within-Module Degree Z-score). This visualization was obtained using BrainNet Viewer [78].

4.2. Discussion on top predictive features

The study also used the RCE-SVM framework to pick out the top connectivity and complex network features based on their discriminative ability. Since these were fairly large numbers of features for the final cluster providing maximum accuracy (147 FC features, 115 complex network features and 347 features in the combined feature set comprising of 320 FC and 27 graph measures), we imposed an additional constraint of high statistical significance (ASD vs. controls, $p < 0.05$, corrected for multiple comparisons using the false discovery rate

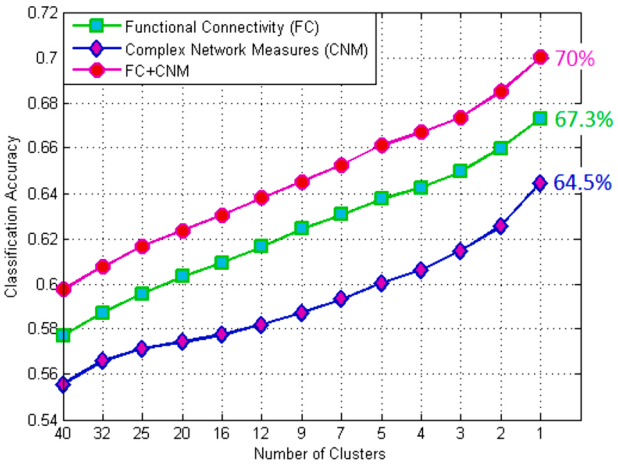

Fig. 3. Machine learning classification was performed using RCE-SVM classifier, to classify between ASD and control groups. Figure shows mean classification accuracies across RCE iterations. Classification was performed independently for three different choices of feature sets: (i) Functional connectivity values computed using Pearson correlation (green line). (ii) Complex network features extracted from functional connectivity values (blue line). (iii) Both functional connectivity and complex network features taken together (pink line). We observed that using complex network features along with functional connectivity values as features led to improved classification accuracy.

Table 5
Machine learning classification was done using RCE-SVM, to classify between controls and individuals with ASD. Table provides mean classification accuracies along with corresponding p-values of comparison.

Feature set	Accuracy	p-Values
Functional connectivity	67.31 %	
Complex network features	64.47 %	FC vs. complex network: 3.3×10^{-62}
FC and complex network features combined	70.01 %	FC + complex network vs. FC: 4.5×10^{-61}

method). This provided 13 features for the FC classifier (Table 2), 8 features for the complex network classifier (Table 3) and 16 features for the combined classifier (out of which 15 were FC features and one was a complex network feature). This hints at why we might have observed higher accuracy by 3 % using connectivity features compared to graph features, as there were more top discriminative connectivity features. However, the addition of the 27 additional complex network features (including the "Within-Module Degree Z-score" for the left precuneus) to the 320 FC features provided additional predictive power of 3 %. This demonstrates the utility of combining connectivity and complex network measures for ASD classification.

We can also observe that the top features were generally associated with brain networks that have been previously found to be impaired in ASD [33,34]. For example, it is evident from Fig.2 that communication between prefrontal, lateral temporal and parietal (especially precuneus) cortices were most discriminative between the groups. Communication between these regions are generally known to support social and linguistic cognition, which is impaired in ASD [36,65]. There is also broad agreement between discriminative features obtained from the three feature sets (broadly implicating the fronto-temporal-parietal axis). Further, connections were mostly weaker in ASD compared to the control group, although limited local hyper-connectivity in ASD was noticed within the orbito-frontal regions. This is in agreement with the general consensus that characterizes ASD as a developmental disconnection syndrome [79].

4.3. Limitations

Our study must be viewed in light of some limitations. Although our data set was relatively large compared to conventional fMRI studies, generalizing the findings to the general society mandates studies on much larger samples. Our data set was a conglomerate of data from multiple sites, with data obtained from different scanners that were not harmonized and used different imaging protocols. This adds undesirable variance to the data that would impair the classification performance; hence, we cannot be sure about the true accuracy we might have obtained if such sources of machine variability had not existed. Variable imaging protocols also have other negative effects; for example, fMRI data obtained with a larger TR irrecoverably loses some information as compared to data with faster TR [80]. Given that ABIDE data set had data with different TRs from different sites, we are not sure how it impacted our final classification performance, and the comparisons that followed.

4.4. Open research questions and future work

Driven by the current study, future work could probe several research questions such as (i) whether adding other types of fMRI measures to the feature set (e.g. dynamic connectivity, effective connectivity) would further enhance the classification accuracy, (ii) whether our finding of better prediction with the combined feature set replicates in other psychiatric and neurological disorders, (iii) whether our findings replicate in other ASD datasets such as the second release of ABIDE (ABIDE-2) and smaller data sets owned by certain investigators, and finally (iv) whether these findings could translate to clinical practice through clinical trials of fMRI in ASD.

Future studies could also undertake the work on much larger datasets than the one used in the current study. Data can be collected from harmonized scanners across sites with the same imaging protocols, which in turn would give true accuracy in the absence of machine variability and different TRs. We believe such an effort has not yet been undertaken to study the ASD population and hence pose as a promising future study. Despite the limitations of our study, we believe our work has implications for future research and we hope that researchers would use superior combined feature sets in the future while studying brain imaging data to diagnose mental disorders.

5. Conclusion

We concluded that complex network measures contain, at least in part, unique information compared to FC. Future studies could combine multiple feature sets arising from different modalities or from different analysis strategies, with the hypothesis that such a conglomeration provides superior prediction performance, supported by findings from our study. Specifically, combining both connectivity and graph measures was demonstrated to diagnose ASD better than using them in isolation. This was seen with the classification accuracies obtained using three different set of features; connectivity features, graph measures, and combined feature set comprising of both connectivity and graph measures. Connectivity alone resulted in 67.31 % classification accuracy in diagnosing ASD vs. controls and graph measures gave 64.47 % accuracy. However, the combined feature set resulted in classification accuracy of 70.01 %.

Future studies could also compare the performance of such feature sets using multiple machine learning techniques to determine the best combination of features and machine learning technique for the diagnosis of ASD. We believe such studies would have translational value and might one day find use in the clinic for objective diagnosis of ASD. Future studies could also test the efficacy of such approaches in the study of other psychiatric and neurologic disorders.

Declaration of competing interests

The authors declare that they have no known competing financial interests or personal relationships that could have appeared to influence the work reported in this paper.

CRediT authorship contribution statement

N. Chaitra: Writing - original draft, Data curation, Visualization, Investigation, Software. **P.A. Vijaya:** Validation, Supervision, Writing - review & editing. **Gopikrishna Deshpande:** Conceptualization, Investigation, Methodology, Writing - review & editing.

Acknowledgments

We thank the ABIDE consortium for publicly providing the large dataset and permitting our use of the ABIDE preprocessed dataset [64]. We are grateful to Dr. Rangaprakash Deshpande (Athinoula A. Martinos Center for Biomedical Imaging, Massachusetts General Hospital, Harvard Medical School and Massachusetts Institute of Technology, Boston, MA, USA) for useful discussions and inputs. The authors are grateful to the authorities of Visvesvaraya Technological University, Belagavi, India and BNM Institute of Technology, Bangalore, India for their encouragement and support extended to carry out this research work.

References

[1] GBD 2015 Disease and Injury Incidence and Prevalence Collaborators, Global, regional, and national incidence, prevalence, and years lived with disability for 310 diseases and injuries, 1990–2015: a systematic analysis for the Global Burden of Disease Study 2015, Lancet (London, England) 388 (10053) (2016) 1545–1602.
[2] E. London, The role of the neurobiologist in redefining the diagnosis of autism, Brain Pathol. 17 (October (4)) (2007) 408–411.
[3] N.J. Minshew, D.L. Williams, The new neurobiology of autism, Arch. Neurol. 64 (July (7)) (2007) 945.
[4] M.E. Vissers, M.X. Cohen, H.M. Geurts, Brain connectivity and high functioning autism: a promising path of research that needs refined models, methodological convergence, and stronger behavioral links, Neurosci. Biobehav. Rev. 36 (January (1)) (2012) 604–625.
[5] M.A. Just, Cortical activation and synchronization during sentence comprehension in high-functioning autism: evidence of underconnectivity, Brain 127 (June (8)) (2004) 1811–1821.
[6] M.A. Just, V.L. Cherkassky, T.A. Keller, N.J. Minshew, Cortical activation and synchronization during sentence comprehension in high-functioning autism: evidence of underconnectivity, Brain 127 (June (8)) (2004) 1811–1821.
[7] M.E. Villalobos, A. Mizuno, B.C. Dahl, N. Kemmotsu, R.-A. Müller, Reduced functional connectivity between V1 and inferior frontal cortex associated with visuomotor performance in autism, Neuroimage 25 (April (3)) (2005) 916–925.
[8] D.E. Welchew, et al., Functional disconnectivity of the medial temporal lobe in Asperger's syndrome, Biol. Psychiatry 57 (May (9)) (2005) 991–998.
[9] J.S. Anderson, Cortical underconnectivity hypothesis in autism: evidence from functional connectivity MRI. Comprehensive Guide to Autism, Springer New York, New York, NY, 2014, pp. 1457–1471.
[10] V.L. Cherkassky, R.K. Kana, T.A. Keller, M.A. Just, Functional connectivity in a baseline resting-state network in autism, Neuroreport 17 (November (16)) (2006) 1687–1690.
[11] D.P. Kennedy, E. Courchesne, The intrinsic functional organization of the brain is altered in autism, Neuroimage 39 (February (4)) (2008) 1877–1885.
[12] A. Di Martino, et al., The autism brain imaging data exchange: towards large-scale evaluation of the intrinsic brain architecture in autism HHS public access, Mol. Psychiatry 19 (6) (2014) 659–667.
[13] S.J. Gotts, W.K. Simmons, L.A. Milbury, G.L. Wallace, R.W. Cox, A. Martin, Fractionation of social brain circuits in autism spectrum disorders, Brain 135 (September (9)) (2012) 2711–2725.
[14] E.A.H. von dem Hagen, R.S. Stoyanova, S. Baron-Cohen, A.J. Calder, Reduced functional connectivity within and between 'social' resting state networks in autism spectrum conditions, Soc. Cogn. Affect. Neurosci. 8 (August (6)) (2013) 694–701.
[15] H. Koshino, P.A. Carpenter, N.J. Minshew, V.L. Cherkassky, T.A. Keller, M.A. Just, Functional connectivity in an fMRI working memory task in high-functioning autism, Neuroimage 24 (February (3)) (2005) 810–821.
[16] I. Dinstein, et al., Disrupted neural synchronization in toddlers with autism, Neuron 70 (June (6)) (2011) 1218–1225.
[17] J.S. Anderson, et al., Decreased interhemispheric functional connectivity in autism, Cereb. Cortex 21 (May (5)) (2011) 1134–1146.
[18] J.S. Anderson, et al., Functional connectivity magnetic resonance imaging classification of autism, Brain 134 (December (12)) (2011) 3742–3754.
[19] R.A. Müller, P. Shih, B. Keehn, J.R. Deyoe, K.M. Leyden, D.K. Shukla, Underconnected, but how? A survey of functional connectivity MRI studies in autism Spectrum disorders, Cereb. Cortex 21 (October (10)) (2011) 2233–2243.
[20] J.M. Tyszka, D.P. Kennedy, L.K. Paul, R. Adolphs, Largely typical patterns of resting-state functional connectivity in high-functioning adults with autism, Cereb. Cortex 24 (July (7)) (2014) 1894–1905.
[21] A. Di Martino, et al., Aberrant striatal functional connectivity in children with autism, Biol. Psychiatry 69 (May (9)) (2011) 847–856.
[22] B. Keehn, P. Shih, L.A. Brenner, J. Townsend, R.-A. Müller, Functional connectivity for an 'Island of sparing' in autism spectrum disorder: an fMRI study of visual search, Hum. Brain Mapp. 34 (October (10)) (2013) 2524–2537.
[23] J.S. Anderson, et al., Abnormal brain synchrony in down syndrome, Neuroimage Clin. 2 (2013) 703–715.
[24] C.J. Lynch, L.Q. Uddin, K. Supekar, A. Khouzam, J. Phillips, V. Menon, Default mode network in childhood autism: posteromedial cortex heterogeneity and relationship with social deficits, Biol. Psychiatry 74 (August (3)) (2013) 212–219.
[25] M. Rubinov, O. Sporns, Complex network measures of brain connectivity: uses and interpretations, Neuroimage 52 (September (3)) (2010) 1059–1069.
[26] D. Rangaprakash, M.N. Dretsch, J.S. Katz, T.S. Denney, G. Deshpande, Dynamics of segregation and integration in directional brain networks: illustration in soldiers with PTSD and neurotrauma, Front. Neurosci. 13 (2019) 803.
[27] M.D. Wheelock, D. Rangaprakash, N.G. Harnett, K.H. Wood, T.R. Orem, S. Mrug, D. A. Granger, G. Deshpande, D.C. Knight, Psychosocial stress reactivity is associated with decreased whole brain network efficiency and increased amygdala centrality, Behav. Neurosci. 132 (6) (2018) 561–572.
[28] Danielle S. Bassett, Nicholas F. Wymbs, Mason A. Porter, Peter J. Mucha, Jean M. Carlson, Scott T. Grafton, Dynamic reconfiguration of human brain networks during learning, PNAS 108 (May (18)) (2011) 7641–7646.
[29] Martin Grandjean, A social network analysis of twitter: mapping the digital humanities community, in: Cogent Arts & Humanities, 3, 2016, 1171458.
[30] Ankush Kumar, G.U. Kulkarni, Evaluating conducting network based transparent electrodes from geometrical considerations, J. Appl. Phys. 119 (2016) 015102.
[31] R.C. Craddock, G.A. James, P.E. Holtzheimer, X.P. Hu, H.S. Mayberg, A whole brain fMRI atlas generated via spatially constrained spectral clustering, Hum. Brain Mapp. 33 (August (8)) (2012) 1914–1928.
[32] X. Bi, Y. Wang, Q. Shu, Q. Sun, Q. Xu, Classification of autism spectrum disorder using random support vector machine cluster, Front. Genet. 9 (February) (2018) 18.
[33] Masoumeh Sadeghi, Reza Khosrowabadi, Fatemeh Bakouie, Hoda Mahdavi, Changiz Eslahchi, Hamidreza Pouretemad, Screening of autism based on task-free fMRI using graph theoretical approach, Psychiatry Res Neuroimaging 263 (May) (2017) 48–56.
[34] Amirali Kazeminejad, Roberto C. Sotero, Topological properties of resting-state fMRI functional networks improve machine learning-based autism classification, Front. Neurosci. 21 (January) (2019) 1018.
[35] D.S. Bassett, E.T. Bullmore, 2009. Human brain networks in health and disease, Curr Opin Neurol. 22 (4) (2009) 340–347, https://doi.org/10.1097/WCO.0b013e32832d93dd.
[36] G. Deshpande, L.E. Libero, K.R. Sreenivasan, H.D. Deshpande, R.K. Kana, Identification of neural connectivity signatures of autism using machine learning, Front. Hum. Neurosci. 7 (2013).
[37] G. Deshpande, Z. Li, P. Santhanam, C.L.M. Coles, S. Hamann, X. Hu, Recursive cluster elimination based support vector machine for disease state prediction using resting state functional and effective brain connectivity, PLoS One 5 (12) (2010).
[38] J.V. Haxby, et al., Distributed and overlapping representations of faces and objects in ventral temporal cortex, Science 293 (5539) (2001) 2425–2430.
[39] A.J. O'Toole, F. Jiang, H. Abdi, J.V. Haxby, Partially distributed representations of objects and faces in ventral temporal cortex, J. Cogn. Neurosci. 17 (April (4)) (2005) 580–590.
[40] A. Buchweitz, S.V. Shinkareva, R.A. Mason, T.M. Mitchell, M.A. Just, Identifying bilingual semantic neural representations across languages, Brain Lang. 120 (3) (2012) 282–289.
[41] T.M. Mitchell, et al., Predicting human brain activity associated with the meanings of nouns, Science 320 (5880) (2008) 1191–1195.
[42] S.V. Shinkareva, V.L. Malave, R.A. Mason, T.M. Mitchell, M.A. Just, Commonality of neural representations of words and pictures, Neuroimage 54 (3) (2011) 2418–2425.
[43] K.S. Kassam, A.R. Markey, V.L. Cherkassky, G. Loewenstein, M.A. Just, Identifying emotions on the basis of neural activation, PLoS One 8 (June (6)) (2013) e66032.
[44] Y. Wang, V. Chattaraman, H.J. Kim, G. Deshpande, Predicting purchase decisions based on spatio-temporal functional MRI features using machine learning, IEEE Trans. Cogn. Dev. Syst. 7 (3) (2015) 248–255.
[45] G. Bellucci, T. Hahn, G. Deshpande, F. Krueger, Functional connectivity of specific resting state networks predicts trust and reciprocity in the trust game, Cogn. Affect. Behav. Neurosci. 132 (6) (2018) 561–572.
[46] A.J. Bauer, M.A. Just, Monitoring the growth of the neural representations of new animal concepts, Hum. Brain Mapp. 36 (August (8)) (2015) 3213–3226.
[47] J. Yang, et al., Common SNPs explain a large proportion of the heritability for human height, Nat. Genet. 42 (July (7)) (2010) 565–569.
[48] R.C. Craddock, P.E. Holtzheimer, X.P. Hu, H.S. Mayberg, Disease state prediction from resting state functional connectivity, Magn. Reson. Med. 62 (December (6)) (2009) 1619–1628.
[49] D. Rangaprakash, G. Deshpande, T.A. Daniel, A.M. Goodman, J.L. Robinson, N. Salibi, J.S. Katz, T.S. Denney, M.N. Dretsch, Compromised hippocampus-striatum pathway as a potential imaging biomarker of mild traumatic brain injury and post-traumatic stress disorder, Hum. Brain Mapp. 38 (6) (2017) 2843–2864.

[50] C. Jin, H. Jia, P. Lanka, D. Rangaprakash, L. Li, T. Liu, X. Hu, G. Deshpande, Dynamic brain connectivity is a better predictor of PTSD than static connectivity, Hum. Brain Mapp. 38 (9) (2017) 4479–4496.
[51] M.A. Syed, Z. Yang, D. Rangaprakash, X. Hu, M.N. Dretsch, J. Katz, T.S. Denney, G. Deshpande, DisConICA: a software package for assessing reproducibility of brain networks and their discriminability across disorders, Neuroinformatics 18 (1) (2020) 7–107.
[52] M. Syed, Z. Yang, X. Hu, G. Deshpande, Investigating brain connectomic alterations in autism using the reproducibility of independent components derived from resting state functional MRI data, Front. Neurosci. 11 (2017) 459.
[53] J.A. Nielsen, et al., Multisite functional connectivity MRI classification of autism: ABIDE results, Front. Hum. Neurosci. 7 (2013) 599.
[54] A. Abraham, et al., Deriving reproducible biomarkers from multi-site resting-state data: an Autism-based example, Neuroimage 147 (February) (2017) 736–745.
[55] I. Gori, et al., Gray matter alterations in young children with autism spectrum disorders: comparing morphometry at the voxel and regional level, J. Neuroimaging 25 (November (6)) (2015) 866–874.
[56] Y. Jin, et al., Identification of infants at high-risk for autism spectrum disorder using multiparameter multiscale white matter connectivity networks, Hum. Brain Mapp. 36 (December (12)) (2015) 4880–4896.
[57] H. Chen, et al., Multivariate classification of autism spectrum disorder using frequency-specific resting-state functional connectivity—a multi-center study, Prog. Neuro-Psychopharmacol. Biol. Psychiatry 64 (January) (2016) 1–9.
[58] P. Odriozola, L.Q. Uddin, C.J. Lynch, J. Kochalka, T. Chen, V. Menon, Insula response and connectivity during social and non-social attention in children with autism, Soc. Cogn. Affect. Neurosci. 11 (March (3)) (2016) 433–444.
[59] G. Chanel, S. Pichon, L. Conty, S. Berthoz, C. Chevallier, J. Grèzes, Classification of autistic individuals and controls using cross-task characterization of fMRI activity, Neuroimage Clin. 10 (2015) (2016) 78–88.
[60] A.S. Heinsfeld, A.R. Franco, R.C. Craddock, A. Buchweitz, F. Meneguzzi, Identification of autism spectrum disorder using deep learning and the ABIDE dataset, Neuroimage Clin. 17 (January) (2018) 16–23.
[61] L.E. Libero, T.P. DeRamus, A.C. Lahti, G. Deshpande, R.K. Kana, Multimodal neuroimaging based classification of autism spectrum disorder using anatomical, neurochemical and white matter correlates, Cortex 66 (2015) 46–59.
[62] P. Lanka, D. Rangaprakash, M.N. Dretsch, J.S. Katz, T.S. Denney, G. Deshpande, Supervised machine learning for diagnostic classification from large-scale neuroimaging datasets, Brain Imaging Behav. (2019) [published online ahead of print, 2019 Nov 5].
[63] P. Lanka, D. Rangaprakash, S.S.R. Gotoor, M.N. Dretsch, J.S. Katz, T.S. Denney, G. Deshpande, MALINI (machine learning in neuroimaging): a MATLAB toolbox for aiding clinical diagnostics using resting-state fMRI data, Data Brief (2020) (Published 2020 Jan 31).
[64] C. Craddock, et al., The Neuro Bureau Preprocessing Initiative: open sharing of preprocessed neuroimaging data and derivatives, Front. Neuroinform. 7 (2013).
[65] A. Di Martino, et al., The autism brain imaging data exchange: towards a large-scale evaluation of the intrinsic brain architecture in autism, Mol. Psychiatry 19 (June (6)) (2014) 659–667.
[66] D.A. Handwerker, J.M. Ollinger, M. D'Esposito, Variation of BOLD hemodynamic responses across subjects and brain regions and their effects on statistical analyses, Neuroimage 21 (April (4)) (2004) 1639–1651.
[67] D. Rangaprakash, G.-R. Wu, D. Marinazzo, X. Hu, G. Deshpande, Hemodynamic response function (HRF) variability confounds resting-state fMRI functional connectivity, Magn. Reson. Med. 80 (October (4)) (2018) 1697–1713.
[68] D. Rangaprakash, G.-R. Wu, D. Marinazzo, X. Hu, G. Deshpande, Parameterized hemodynamic response function data of healthy individuals obtained from resting-state functional MRI in a 7T MRI scanner, Data Brief 17 (2018) 1175–1179.
[69] D. Rangaprakash, M.N. Dretsch, W. Yan, J.S. Katz, T.S. Denney, G. Deshpande, Hemodynamic variability in soldiers with trauma: Implications for functional MRI connectivity studies, Neuroimage Clin. 16 (2017) 409–417.
[70] D. Rangaprakash, M.N. Dretsch, W. Yan, J.S. Katz, T.S. Denney, G. Deshpande, Hemodynamic response function parameters obtained from resting-state functional MRI data in Soldiers with trauma, Data Brief 14 (2017) 558–562.
[71] W. Yan, D. Rangaprakash, G. Deshpande, Aberrant hemodynamic responses in autism: implications for resting state fMRI functional connectivity studies, Neuroimage Clin. 19 (2018) 320–330.
[72] W. Yan, D. Rangaprakash, G. Deshpande, Hemodynamic response function parameters obtained from resting state BOLD fMRI data in subjects with autism spectrum disorder and matched healthy controls, Data Brief 14 (2017) 558–562.
[73] G.-R. Wu, W. Liao, S. Stramaglia, J.-R. Ding, H. Chen, D. Marinazzo, A blind deconvolution approach to recover effective connectivity brain networks from resting state fMRI data, Med. Image Anal. 17 (April (3)) (2013) 365–374.
[74] R. Guimerà, L.A.N. Amaral, Cartography of complex networks: modules and universal roles, J. Stat. Mech. 2005 (February (P02001)) (2005) p. nihpa35573.
[75] D.J. Watts, S.H. Strogatz, Collective dynamics of 'small-world' networks, Nature 393 (June (6684)) (1998) 440–442.
[76] V. Latora, M. Marchiori, Efficient behavior of small-world networks, Phys. Rev. Lett. 87 (October (19)) (2001) 198701.
[77] M. Yousef, S. Jung, L.C. Showe, M.K. Showe, Recursive cluster elimination (RCE) for classification and feature selection from gene expression data, BMC Bioinformatics 8 (May (1)) (2007) 144.
[78] M. Xia, J. Wang, Y. He, BrainNet viewer: a network visualization tool for human brain connectomics, PLoS One 8 (7) (2013).
[79] Daniel H. Geschwind, Pat Levitt, Autism spectrum disorders: developmental disconnection syndromes, Curr. Opin. Neurobiol. 17 (February (1)) (2007) 103–111.
[80] Amy R. McDowell, David W. Carmichael, Optimal repetition time reduction for single subject event-related functional magnetic resonance imaging, Magn. Reson. Med. 81 (September (3)) (2019) 1890–1897.